

LEFT-HANDED MATERIALS BASED ON CRYSTAL LATTICE VIBRATION

R. Wang and J. Zhou

State Key Laboratory of New Ceramics and Fine Processing
Department of Materials Science and Engineering
Tsinghua University, Beijing 100084, China

C.-Q. Sun

School of Electrical and Electronic Engineering
Nanyang Technological University
Singapore 639798, Singapore

L. Kang

State Key Laboratory of New Ceramics and Fine Processing
Department of Materials Science and Engineering
Tsinghua University, Beijing 100084, China

Q. Zhao

State Key Laboratory of Tribology
Department of Precision Instruments and Mechanology
Tsinghua University
Beijing 100084, China

J.-B. Sun

State Key Laboratory of New Ceramics and Fine Processing
Department of Materials Science and Engineering
Tsinghua University, Beijing 100084, China

Abstract—An all-dielectric composite route is proposed for the construction of a left-handed material at THz frequency. It is shown that the interaction between the crystal lattice vibration of the polaritonic dielectric and the electromagnetic wave could

induce a negative permittivity. By combining the electric inclusion of polaritonic dielectric with the magnetic inclusion based on Mie resonance, the dielectric composite exhibits simultaneously negative permittivity and negative permeability, hence a negative refractive index. Additionally, the simulation results of the electromagnetic coupling between the electric and magnetic inclusions indicate that the behavior of the negative refractive index is closely related to the distance between the two inclusions.

1. INTRODUCTION

Negative refraction in the left-hand materials (LHMs) with negative permittivity and negative permeability simultaneously has attracted much attention for their exotic electromagnetic (EM) properties [1–7]. Due to the fact that natural materials with both negative permittivity and negative permeability have not been available, the conventional LHMs have focused on the combination of subwavelength metallic structures to achieve negative parameters at the same time by electric and magnetic resonances, and thus a negative refractive index [2–6]. For instance, the combination of split ring resonators (SRRs) and metallic wires is widely adopted [2–4]. In this case, the SRRs provide the negative effective permeability based on magnetic resonance which depends on its detailed geometry, while the metallic wires provide the negative effective permittivity when the frequency below the plasmon frequency. However, these artificial materials mainly gain their negative parameters from the structures rather than from their intrinsic properties directly. It should be a big challenge to realize them in optical frequency due to much complicated nano-fabrication technique. So it will be very interesting and significant to realize nonmetallic LHMs using the intrinsic properties of the materials.

Although substances with both negative permittivity and negative permeability are absent in natural materials, to realize the negative permeability and the negative permittivity respectively with natural materials is still possible. Recently, the magnetic resonator has been upgraded from SRRs to dielectric particles ($\text{Sr}_{0.5}\text{Ba}_{0.5}\text{TiO}_3$, LiTaO_3 and SiC) with high permittivity based on the Mie theory at microwave and infrared frequencies [7–12]. Moreover, if the sphere radius is increased, such particles can also exhibit an electric resonance in the same frequency range [13, 14]. Therefore, a LHM can be realized by using dielectric spheres of two distinct sizes or combining dielectric particles with metallic wires. Besides, ferrites or magnetic metals may also possess a negative permeability at certain frequency by the ferromagnetic resonance [15, 16].

A difficulty to realize all-dielectric LHMs is the negative permittivity inclusions. As the electric resonance in Mie particles is the second one, the resonance is relative weak and hard to be negative, especially in high frequency to infrared range. In this work, we proposed a new mechanism to realize negative permittivity, which is based on crystal lattice vibration of the polaritonic dielectrics. In combination with the negative effective permeability based on Mie resonance, a negative refractive index is expected to be generated.

2. ELECTRIC INCLUSION

Classic theory of lattice dynamics [17] has shown that, the relative permittivity of polaritonic dielectrics will exhibit one or more electric resonances near the transverse optical phonon frequencies due to the excitation of transverse optical phonons by lattice vibration at the infrared regime. At frequencies just above the transverse optical phonon vibration, the relative permittivity is negative.

For polaritonic materials, the lattice vibration at the infrared frequency can be expected to tailor permittivity resonance. For single oscillator (transverse vibrational mode), the dielectric dispersion relation of polaritonic materials can be expressed as [17]

$$\varepsilon(\omega) = \varepsilon_{\infty} + \frac{(\varepsilon_0 - \varepsilon_{\infty})\omega_T^2}{\omega_T^2 - \omega^2 + i\omega\gamma} \quad (1)$$

where ε_{∞} is the high-frequency dielectric constant, ε_0 is the static permittivity, ω_T is the transverse optical phonon frequency and γ is the damping coefficient. It has the same form to that of the classic Lorentz dispersion relation. The CaTiO_3 (CTO) ceramic, which is well known as mineral perovskite, is chosen to act as the electric inclusion, and it has three vibration modes [18]: a cation- TiO_3 lattice vibration mode at 110 cm^{-1} ($\sim 3.3 \text{ THz}$), a T-O bending mode at 170 cm^{-1} ($\sim 5 \text{ THz}$) and a T-O stretching mode at 550 cm^{-1} ($\sim 16.5 \text{ THz}$). Resonances of the latter two vibration modes are much weaker than the one at about 3.3 THz . Therefore, to simplify the calculation, we ignore the influence of the two vibration modes at higher frequencies and fit to the dielectric data taken from the reported experimental results [19] by using Eq. (1). The fitted model parameters are given as follows: $\varepsilon_0 = 190$, $\varepsilon_{\infty} = 5.6$, $\omega_T/2\pi = 3.3 \text{ THz}$ and $\gamma/2\pi = 0.8 \text{ THz}$. Figure 1(a) shows the dielectric dispersion curves of the CTO bulk.

Although the CTO ceramic exhibits threefold degenerate vibration modes and isotropic dielectric dispersion due to its cubic (space group pm3m) crystal structure, it is still designed as rod-shape in this paper not only for the enhancement of the electric response but also for

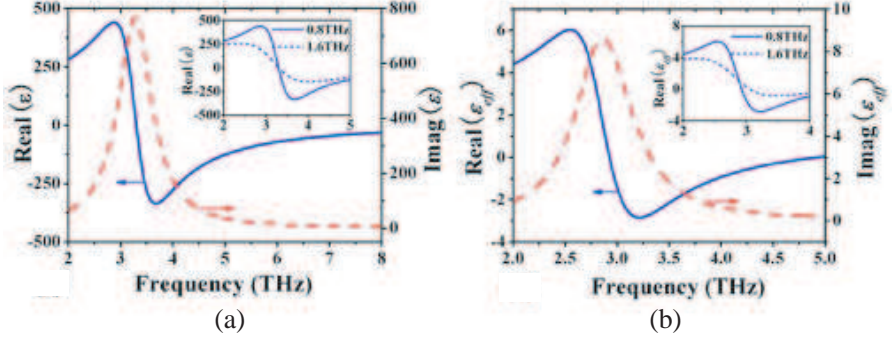


Figure 1. (a) The fitted dispersion curves of CTO bulk using single oscillator model. (b) The effective permittivity of the CTO rods with the cross sectional area $1 \times 1 \mu\text{m}^2$ and the infinite length. The unit dimension is $10 \mu\text{m}$ and the electric field \mathbf{E} polarizes along the axis of the rod. Insets show the results with different γ values. (solid line: $\gamma/2\pi = 0.8 \text{ THz}$, dashed line: $\gamma/2\pi = 1.6 \text{ THz}$).

ensuring enough space to degenerate the EM interaction between electric and magnetic inclusions. The effective permittivity (ϵ_{eff}) of the CTO rods with the cross sectional area $1 \times 1 \mu\text{m}^2$ and infinite length is calculated based on the effective medium theory [20] and the results are shown in Figure 1(b). The electric field \mathbf{E} polarizes along the axis of the rod and the lattice constant is $10 \mu\text{m}$. It can be seen from Figure 1(b) that, due to the low filling fraction (1%), the ϵ_{eff} of the CTO rods is much smaller than that of the bulk. Nevertheless, the negative permittivity is still realized above 2.92 THz and the minimum real value of the ϵ_{eff} approaches to -3 at about 3.2 THz.

It has been reported that the electric resonance of dielectric rod-shaped particles with high permittivity can also be excited by Mie resonance [10]. If the resonant model ϵ_{eff} of the CTO rods arises from Mie resonance, the position of the resonant peak should shift towards a higher frequency with decreasing the permittivity of the bulk material [13]. Therefore, in order to prove that the resonant model ϵ_{eff} of the CTO rods results from the intrinsic dielectric property rather than Mie resonance, we increase the damping coefficient $\gamma/2\pi$ from 0.8 THz to 1.6 THz to reduce the oscillator strength in CTO (dotted line in Figure 1(a) inset), and thus the bulk permittivity. The calculated ϵ_{eff} of the CTO rods with the same size but different $\gamma/2\pi$ values are shown in the inset of Figure 1(b). The results indicate that the peak position of the resonant permittivity is unchanged, only the

strength of the resonance weakens as the bulk permittivity decreases. This distinctly verifies that the negative permittivity originates from the lattice vibration, i.e., from the intrinsic property of CTO ceramic.

3. MAGNETIC INCLUSION

For the magnetic inclusion, a collection of LiTaO_3 (LT) dielectric spheres is considered. The relative permittivity of LT bulk exhibits a sharp resonance near 4.25 THz by the lattice vibration and the dielectric dispersion function of LT bulk satisfies the form in Eq. (1) as well. The parameters used are given as follows: $\epsilon_0 = 41.4$, $\epsilon_\infty = 13.4$, $\omega_T/2\pi = 4.25$ THz and $\gamma/2\pi = 0.15$ THz. The complex dielectric function of LT bulk is presented in Figure 2(a).

For the large permittivity of LT bulk in the frequency region below 4.25 THz, a negative effective permeability (μ_{eff}) can be generated based on Mie theory with suitable particle size [9]. The μ_{eff} of a collection of LT spheres is shown in Figure 2(b), which is obtained based on the effective medium theory [20]. The radius of the sphere is $4\ \mu\text{m}$ and the lattice constant is still $10\ \mu\text{m}$. The results reveal a resonance in μ_{eff} at about 3.53 THz and, in the frequency range just above the resonance, the μ_{eff} is negative and the minimum real value is about -0.26 at 3.58 THz. The same results are also reported previously in Ref. [9]. From the results of the effective parameters in Figure 1(b) and Figure 2(b), it can be seen that the negative regions overlap partially in the frequency range of 3.56–3.64 THz.

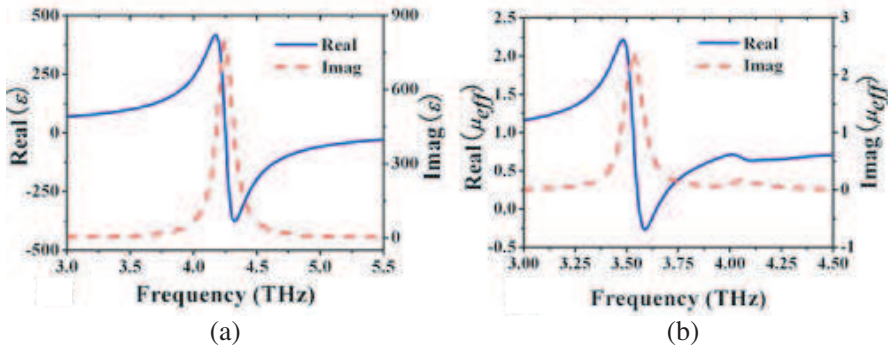


Figure 2. (a) The dielectric function of LT bulk using single oscillator model. (b) The effective permeability of a collection of LT spheres. The radius of the sphere is $4\ \mu\text{m}$ and the lattice constant is $10\ \mu\text{m}$.

4. COMPOSITE LHM

4.1. Simulations and Results

To configure the negative refractive index, we put a CTO rod at both sides of a LT sphere symmetrically, and the space between the CTO rod and the LT sphere is $0.5 \mu\text{m}$. The polarization of the magnetic field is along the z axis and that of the electric field is along the y axis (as shown in Figure 3(a) inset). The transmission coefficients of the CTO rods only, the LT spheres only and the combined medium are simulated using CST microwave studio and the results are shown in Figure 3(a). The CTO rods have a negative permittivity within a wide range as explained in Section 2. As a result, the EM wave cannot propagate in such a medium and a wide forbidden region of the transmission appears accordingly (black dashed line). For the LT spheres only,

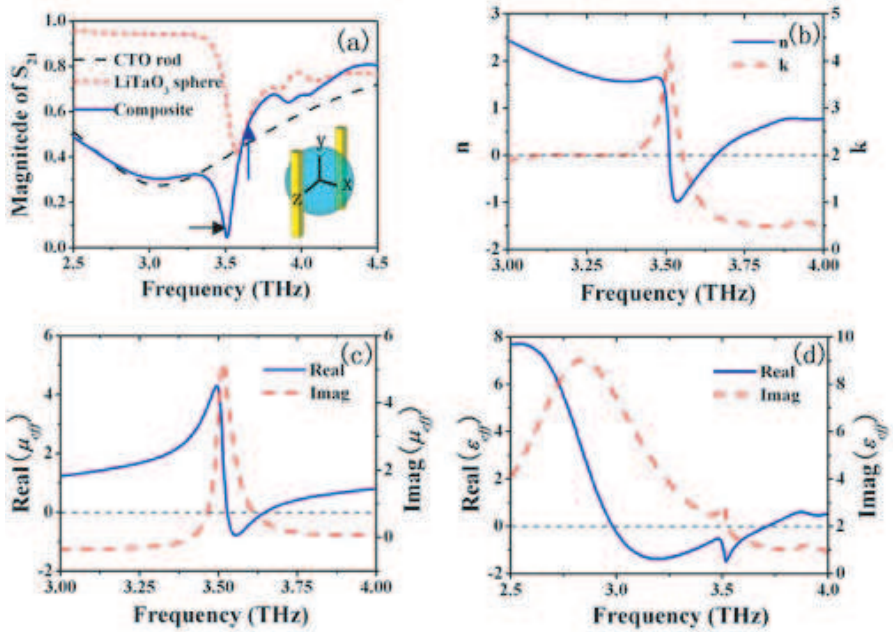


Figure 3. (a) Simulated transmission of the CTO rods only (dashed line), LT spheres only (dotted line), and the combination of them (solid line). Inset shows the orientation of the CTO rods and the LT sphere. Retrieved refractive index (b), effective permeability (c) and effective permittivity (d) of the composite based on the simulated scattering parameters.

there is also a forbidden band that appears around 3.5 THz arising from Mie resonance. By combining the CTO rods with the LT spheres, a passband as marked with the blue arrow in Figure 3(a) is observed around the overlap of the forbidden bands of the LT spheres and the CTO rods.

In order to calculate the effective parameters, the scattering parameters (S_{11} and S_{21}) of only one unit along the propagation direction are simulated. The effective EM parameters are retrieved using the method as described in Ref. [21] and the results are shown in Figures 3(b)–(d). It is noted that the negative refractive index is indeed realized in the range from 3.51 to 3.64 THz as shown in Figure 3(b), which is slightly wider than that of the negative permeability of the LT spheres only (3.56 to 3.64 THz). The wider negative index ranging from 3.51 to 3.56 THz is due to the single negative effective parameter (negative ε_{eff} and positive μ_{eff}) and the large imaginary part of the μ_{eff} near the resonance [22]. Therefore, the negative refractive index in this region (3.51–3.56 THz) is not a result of the left-handed behavior. When the frequency decreases below 3.51 THz, the imaginary part of the μ_{eff} dropped rapidly and the condition as described in Ref. [22] cannot be satisfied. Hence, a deep dip as marked with the black arrow in Figure 3(a) is caused by the remaining large positive μ_{eff} and the negative ε_{eff} .

4.2. Electromagnetic Coupling

Considering the effect of the EM coupling on the negative refractive index, we change the distance (d) between the electric and magnetic inclusions and simulate the magnetic field intensity distributions of the composite near the magnetic resonance as shown in Figure 4.

As expected from Mie theory, the dielectric sphere is equivalent to a magnetic dipole near the magnetic resonance mode and the magnetic field is mainly localized in the sphere as shown in Figure 4(a). However, when the CTO rods are placed beside the dielectric sphere, the magnetic field distribution is changed. The magnetic field in the gap enhances greatly while that in the sphere decreases as the rod approaches the dielectric sphere. When the distance between the rod and the sphere is reduced to zero, the intensity of the magnetic resonance even decreases by about 15% from about 5.7×10^4 A/m to 4.7×10^4 A/m (Figures 4(b)–(c)). This can be understood through the EM coupling between the electric and magnetic inclusions. When the lattice vibration happens in the CTO rod, a displacement current (I) forms inside the CTO rod along the axis by the relative displacement of the ions with opposite charges along the \mathbf{E} polarized direction resulting from the electric resonance (Figure 4(d) inset), thus an annular

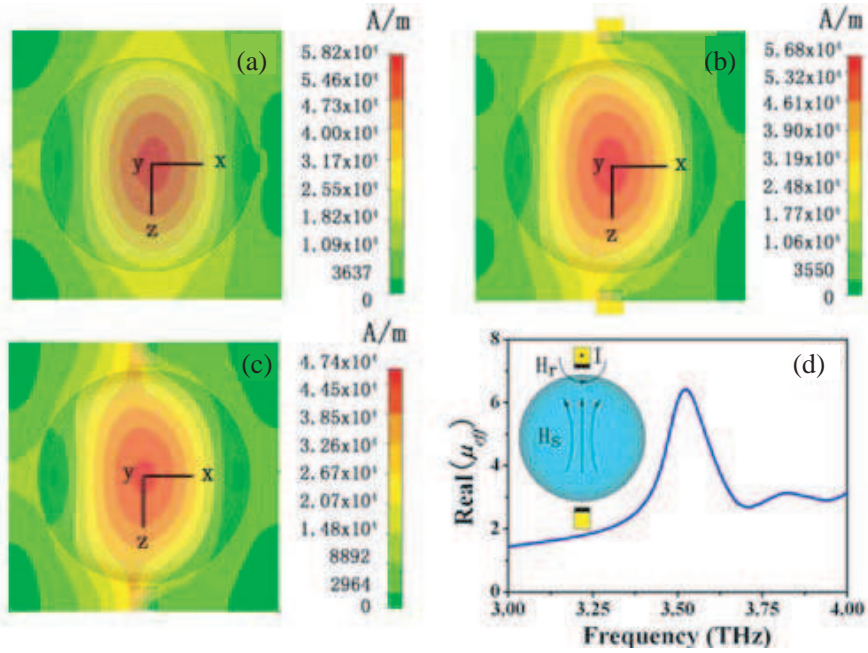


Figure 4. Simulated magnetic field intensity distribution in a LT sphere (a) and in the combination of a LT sphere and two CTO rods with different d value. (b) $d = 0.5 \mu\text{m}$, (c) $d = 0$. (d) The retrieved effective permeability of the combination in (c). Inset is the schematic of the EM coupling between the LT sphere and CTO rods.

magnetic field (\mathbf{H}_r) is induced around the rod. The resonant magnetic field (\mathbf{H}_s) in the dielectric sphere resulting from Mie resonance is along the z axis. As the CTO rod approaches the magnetic resonator, the interaction between them is enhanced dramatically. The annular magnetic field affects on the magnetic resonance and greatly weakens its strength. Moreover, the position of the magnetic resonance shifts towards a higher frequency. Although the effective permeability is still the resonant model, the negative part could not be encountered (Figure 4(d)). Therefore, a suitable distance between the electric and magnetic inclusions is quite significant in the realization of the negative parameters.

From the simulation results discussed above, it has been confirmed that the negative refractive index can be realized by the combination of the electric inclusion based on lattice vibration and the magnetic inclusion based on the Mie resonance. The parameters used for the

simulations are taken or fitted from experimental data and it has more practical applications. Although the negative refractive index is demonstrated only in the THz region, it is possible to extend this design route to the far infrared and even the middle infrared frequency with proper selections of polaritonic materials and particle dimensions. For example, SiC whiskers of $1.5\ \mu\text{m}$ in diameter show a magnetic Mie resonance at about $760\ \text{cm}^{-1}$ [10], while the transverse optical phonon frequency of E_1 mode in BeO single crystal is around $724\ \text{cm}^{-1}$ [23] and the region of the negative permittivity covers the Mie resonance region of SiC whiskers. Moreover, some ferroelectrics such as $\text{Sr}_{0.5}\text{Ba}_{0.5}\text{TiO}_3$ with an electrically tunable property can also be introduced as the electric inclusion and expand the scope of the application [24].

5. CONCLUSION

In summary, we numerically demonstrate a kind of LHMs based on LT dielectric spheres and CTO rods. The left-handed passband is observed in the frequency region where both the effective permeability and permittivity are negative. In this novel design route, the negative permeability is attributed to Mie resonance, while the realization of negative permittivity is no longer using plasmon resonance or electric Mie resonance as described in the previous reports, but the lattice vibration of the polaritonic dielectrics at the transverse optical phonon frequency. The simple nonmetallic structure and an all-dielectric route make it a promising candidate for the LHM design.

ACKNOWLEDGMENT

This work is supported by the National Science Foundation of China under Grants No. 50425204, 50572043, 50621201, 50632030 and 10774087, and Ministry of Education of China.

REFERENCES

1. Veselago, V. G., "The electrodynamics of substances with simultaneously negative values of ϵ and μ ," *Soviet Physics Uspeki*, Vol. 10, 509–514, 1968.
2. Pendry, J. B., "Negative refraction makes a perfect lens," *Phys. Rev. Lett.*, Vol. 85, 3966–3969, 2000.
3. Smith, D. R., W. J. Padilla, D. C. Vier, S. C. Nemat-Nasser, and S. Schultz, "Composite medium with simultaneously negative

- permeability and permittivity,” *Phys. Rev. Lett.*, Vol. 84, 4184–4187, 2000.
4. Houck, A. A., J. B. Brock, and I. L. Chuang, “Experimental observations of a left-handed material that obeys Snell’s law,” *Phys. Rev. Lett.*, Vol. 90, 137401, 2003.
 5. Shalaev, V. M., W. Cai, U. K. Chettiar, H.-K. Yuan, A. K. Sarychev, V. P. Drachev, and A. V. Kildishev, “Negative index of refraction in optical metamaterials,” *Opt. Lett.*, Vol. 30, 3356–3358, 2005.
 6. Padilla, W. J., A. J. Taylor, C. Highstrete, M. Lee, and R. D. Averitt, “Dynamical electric and magnetic metamaterial response at terahertz frequencies,” *Phys. Rev. Lett.*, Vol. 96, 107401, 2006.
 7. Huang, K. C., M. L. Povinelli, and J. D. Joannopoulos, “Negative effective permeability in polaritonic photonic crystals,” *Appl. Phys. Lett.*, Vol. 85, 543, 2004.
 8. O’Brien, S. and J. B. Pendry, “Photonic band-gap effects and magnetic activity in dielectric composites,” *J. Phys.: Condens. Matter*, Vol. 14, 4035–4044, 2002.
 9. Wheeler, M. S., J. S. Aitchison, and M. Mojahedi, “Three-dimensional array of dielectric spheres with an isotropic negative permeability at infrared frequencies,” *Phys. Rev. B*, Vol. 72, 193103, 2005.
 10. Schuller, J. A., R. Zia, T. Taubner, and M. L. Brongersma, “Dielectric metamaterials based on electric and magnetic resonances of silicon carbide particles,” *Phys. Rev. Lett.*, Vol. 99, 107401, 2007.
 11. Peng, L., L. Ran, H. Chen, H. Zhang, J. A. Kong, and T. M. Grzegorzczuk, “Experimental observation of left-handed behavior in an array of standard dielectric resonators,” *Phys. Rev. Lett.*, Vol. 98, 157403, 2007.
 12. Zhao, Q., L. Kang, B. Du, H. Zhao, Q. Xie, X. Huang, B. Li, J. Zhou, and L. Li, “Experimental demonstration of isotropic negative permeability in a three-dimensional dielectric composite,” *Phys. Rev. Lett.*, Vol. 101, 027402, 2008.
 13. Holloway, C. L., E. F. Kuester, J. B. Jarvis, and P. Kabos, “A double negative (DNG) composite medium composed of magnetodielectric spherical particles embedded in a matrix,” *IEEE Trans. Antennas Propag.*, Vol. 51, 2596–2603, 2003.
 14. Vendik, I. B., O. G. Vendik, and M. S. Gashinova, “Artificial dielectric medium possessing simultaneously negative permittivity

- and magnetic permeability,” *Tech. Phys. Lett.*, Vol. 32, 429–433, 2006.
15. Dewar, G., “A thin wire array and magnetic host structure with $n < 0$,” *J. Appl. Phys.*, Vol. 97, 10Q101, 2005.
 16. Chui, S. T. and L. B. Hu, “Theoretical investigation on the possibility of preparing left-handed materials in metallic magnetic granular composites,” *Phys. Rev. B*, Vol. 65, 144407, 2002.
 17. Born, M. and K. Huang, *Dynamical Theory of Crystal Lattices*, Clarendon Press, Oxford, 1954.
 18. Perry, C. H., B. N. Khanna, and G. Rupprecht, “Infrared studies of perovskite titanates,” *Phys. Rev.*, Vol. 135, A408–A412, 1964.
 19. Železny, V., E. Cockayne, J. Petzelt, M. F. Limonov, D. E. Usvyat, V. V. Lemanov, and A. A. Volkov, “Temperature dependence of infrared-active phonons in CaTiO_3 : A combined spectroscopic and first-principles study,” *Phys. Rev. B*, Vol. 66, 224303, 2002.
 20. Bohren, C. F. and D. R. Huffman, *Absorption and Scattering of Light by Small Particles*, Wiley and Sons, New York, 1983.
 21. Smith, D. R., S. Schultz, P. Markos, and C. M. Soukoulis, “Determination of effective permittivity and permeability of metamaterials from reflection and transmission coefficients,” *Phys. Rev. B*, Vol. 65, 195104, 2002.
 22. Zhang, S., W. Fan, N. C. Panoiu, K. J. Malloy, R. M. Osgood, and S. R. J. Brueck, “Experimental demonstration of near-infrared negative-index metamaterials,” *Phys. Rev. Lett.*, Vol. 95, 137404, 2005.
 23. Loh, E., “Optical phonons in BeO crystals,” *Phys. Rev.*, Vol. 166, 673–678, 1968.
 24. Zhao, Q., L. Kang, B. Li, and J. Zhou, “Tunable negative refraction in nematic liquid crystals,” *Appl. Phys. Lett.*, Vol. 89, 221918, 2006.